SUPPLEMENTAL INFORMATION (SI) APPENDIX

Socioeconomic status moderates age-related differences in the brain's functional network organization and anatomy across the adult lifespan

Micaela Y. Chan[1], Jinkyung Na[2], Phillip F. Agres[1],
Neil K. Savalia[1], Denise, C. Park[1,3], & Gagan S. Wig[1,3]

[1]Center for Vital Longevity and School of Behavioral and Brain Sciences, University of Texas at Dallas, Dallas, TX, 75235, USA
[2]Department of Psychology, Sogang University, Seoul, 04107, Korea
[3]Department of Psychiatry, University of Texas Southwestern Medical Center, Dallas, TX, 75390, USA

1. SUPPLEMENTAL RESULTS

1.1. Relationship of income and subjective social-standing to primary measure of Socioeconomic Status (SES), and additional analyses of age-cohort defined SES

For a subset of participants (n=168), additional measures related to SES were available: self-reported income (an objective measure of SES) and social standing (a subjective measure of SES; 1). We examined these measures to determine whether they are related to our primary measure of SES (defined from education and occupational socioeconomic characteristics). The weighted household income of the participants was quantified by identifying the midpoint of a participant's self-report range of household income (the highest earning range [>$500,000] was scaled to 25% above the lower bound [$625,000]), weighted by the square root of the total number of household members, and taking the cube root of the weighted income to normalize the income distribution (2-4).

$$Weighted\ Per\ Capita\ Income = \sqrt[3]{\frac{Household\ Income}{\sqrt[2]{Household\ Members}}}$$

Using the MacArthur's Scale of Subjective Social Standing (1), we measured a participant's subjective SES by presenting him or her with a drawing of a ladder that included 10 rungs, and explained that each rung (level) represents people with different levels of education, income and occupation status. The participants indicated on which rung they believed they stood relative to other people in the United States. A lower score on the MacArthur's scale (higher rung) reflects higher subjective SES.

In the subset of participants with both of these measures, their SES score was correlated with both higher income ($r(166)=0.32$, $p<.001$) as well as higher subjective SES ($r(166)=-0.29$, $p<.001$; smaller values in subjective SES correspond to higher subjective SES).

There is a possibility that SES relates to income and subjective SES differently across age groups. However, no significant interactions were observed between SES and age group on either income ($F(3,160)=0.89$, $p=.445$, $\eta_p^2=.02$) or subjective SES ($F(3,160)=0.93$, $p=.429$, $\eta_p^2=.02$). While the relationships between SES and income or subjective SES do not significantly differ across age groups in the present sample, examining the raw correlation values between income and the main SES measure within each age group revealed that the correlation was strongest in YA and ML (rs>0.43, ps<.032), and weaker in ME and OA (rs<0.31, ps>.120). Subjective SES showed significant negative correlations with the main SES measure in YA, ME and OA (rs<-0.30, ps<.034), but no association in ME ($r(25)=-0.04$, $p=.835$).

Given the minor variation in how SES relates to income and subjective-SES across age group, we tested whether computing the SES score within each respective age group would result in any qualitative differences to the main finding (i.e., the PCA used to extract a factor from education and socioeconomic index were completed within each age group). The resulting age group-specific SES score was strongly correlated with the original SES score ($r(303)=0.99$, $p<.001$). The primary findings regarding the interaction between SES and age on system segregation (β=-0.0003, $t(299)=-2.01$, $p=.046$), and SES by age group on both system segregation ($F(3,295)=3.13$, $p=.026$, $\eta_p^2=.03$) and cortical thickness ($F(3,295)=2.66$, $p=.049$, $\eta_p^2=.03$) remained significant when using the age group-specific SES scores.

1.2. SES-brain relations in different age segments

The relationship between SES and both brain measures in middle-age segments (see **Fig. 2** of main manuscript) parallels previous findings in the literature reporting a positive relationship between SES and cortical thickness (whole-brain and regional) in middle-age adulthood (middle-age adults range: 35-64y (5) and 30-54y (6)). While the age grouping used in the present study was driven by methodological decisions regarding functional network identification and analysis (see main text), we examined the SES-brain relationships across the middle-age range (35-64y). SES significantly predicted brain system segregation (β=0.20, $t(125)=2.24$, $p=.027$) and mean cortical thickness (β=0.19, $t(125)=2.16$, $p=.033$), after accounting for head motion.

In contrast to middle-age adults, younger-age adults did not exhibit significant relationships with either system segregation or mean cortical thickness (ts< 1.85, ps >.071). In the older group, a marginally significant negative relationship between SES and system segregation was noted (β=-0.17, $t(129)=-1.98$, $p=.0501$). The relationship between SES and mean cortical thickness was non-significant in older adults (β=-0.12, $t(129)=-1.32$, $p=.188$).

1.3. Interaction of age group with SES components: education attainment and occupational socioeconomic characteristics

A participant's SES score was composed from their education years and occupational socioeconomic index. To determine whether the individual components forming the SES construct interacted with age differently in relation to the brain's neuroanatomy and functional network organization, each measure was independently examined in relation to age and the brain. GLMs were constructed to examine the effect of education or occupational socioeconomic index, age group, and their interaction on brain system segregation and mean

cortical thickness (ICV-adjusted); in-scanner head motion (mean FD) was entered as a covariate. The main effect of occupational socioeconomic index and education years did not significantly predict either brain variable, consistent with our primary observations that included the composite SES measure. However, the interaction between occupational socioeconomic index and age group significantly predicted both brain system segregation (F(3,295)=2.81, p=.040, η_p^2=.03) and cortical thickness (F(3,295)=2.64, p=.050, η_p^2=.03). Further, these interaction effects remained significant when controlling for education (brain system segregation: F(3,294)=2.78, p=.041, η_p^2=.03; cortical thickness: F(3,294)=2.69, p=.047, η_p^2=.03). Conversely, an interaction between education years and age group significantly predicted brain system segregation (F(3,295)=2.68, p=.047, η_p^2=.03), but not cortical thickness (F(3,295)=1.69, p=.169, η_p^2=.02); and when controlling for occupational socioeconomic index, the interaction remained significant for brain system segregation (F(3,294)=2.66, p=.048, η_p^2=.03). While the two independent variables were correlated (education years and occupational socioeconomic index: r(302)=0.49, p<.001), these observations suggest that the two variables may exhibit unique relationships with brain function and anatomy.

1.4. SES by age (continuous) interaction on system segregation while controlling for additional covariates

A significant interaction between SES and continuous age was observed in brain system segregation. This interaction remained significant when separately controlling for physical health (F(1,292)=4.00, p=.047, η_p^2=.01), episodic memory (F(1,298)=4.07, p=.045, η_p^2=.01), and fluid processing (F(1,298)=4.05, p=.045, η_p^2=.01); the interaction attenuated to a marginal effect when controlling for participant demographics (F(1,288)=2.84, p=.093, η_p^2=.03) and mental health (F(1,296)=-1.95, p=.052, η_p^2=.01).

1.5. Further considerations of the relationship between Childhood-SES and brain measures

As reported in the main manuscript, in models controlling for age group, the childhood-SES to brain relation was not significant. Given the previously reported relationship between an individual's childhood-SES and features of their adult brain (e.g., 7), we explored the simple relationship between childhood-SES and both brain measures while only controlling for head motion in the sub-sample of participants with childhood-SES data (n=168). In statistical models that did not control for age group, childhood-SES was significantly associated with cortical thickness (F(6,160)=2.70, p=.016, η_p^2=.09), while exhibiting a marginal relationship with system

segregation ($F(6,160)=2.11$, $p=.055$, $\eta_p^2=.07$). However, given the significant association between childhood-SES and age group (see main text), where older adults tended to have parents with lower education (see **Table S1**), the associations between childhood-SES and the two brain measures in our present sample are confounded with age.

Age group	N	Education Years (*SD*)	Occupational Socioeconomic Index (*SD*)	Childhood-SES (% of participants)
Younger Adults (20-34y)	25	16.80 (2.40)	49.09 (14.48)	0% Primary School 20% High School 16% Associate's Degree 36% Bachelor's Degree 28% Master's Degree 0% PhD 0% MD
Middle-Early Adults (35-49y)	26	16.48 (2.37)	49.82 (13.60)	0% Primary School 35% High School 4% Associate's Degree 27% Bachelor's Degree 27% Master's Degree 4% PhD 4% MD
Middle-Late Adults (50-64y)	50	15.75 (2.09)	48.92 (11.70)	8% Primary School 38% High School 16% Associate's Degree 26% Bachelor's Degree 4% Master's Degree 4% PhD 4% MD
Older Adults (65-89y)	67	15.57 (2.47)	47.98 (10.37)	24% Primary School 42% High School 10% Associate's Degree 16% Bachelor's Degree 7% Master's Degree 0% PhD 0% MD

Table S1 – Childhood-SES of sub-sample (n=168). Childhood-SES = highest degree completed by either parent of the participant.

1.6. System-specific differences in functional network organization and regional differences in brain anatomy

The central analysis of the main report focuses on global measures of functional network organization (mean brain system segregation) and brain anatomy (mean cortical thickness). Additional follow-up analyses were conducted to further understand the more specific brain differences.

SES-related differences in the segregation of specific types of brain systems

We examined the system segregation of specific types of brain systems (see 8). Functional brain systems were categorized into two distinct systems types: (i) *sensory-motor systems*, which primarily receive and process sensory and motor signals, and (ii) *association systems*, which are typically involved in directing and integrating information across a variety of tasks (9, 10). System segregation can then be calculated to quantify the degree to which different types of systems are segregated from one another (e.g., the segregation of sensory-motor systems from association systems; see **Supplemental Methods** below for details on calculating system segregation for specific systems). These analyses revealed a significant SES by age group interaction on the segregation of association systems from all other brain systems ($F(3,295)=2.76$, $p=.042$, $\eta_p^2=.03$) and on the segregation of association systems from each other ($F(3,295)=3.05$, $p=.029$, $\eta_p^2=.03$). Segregations of sensory-motor systems were not significantly predicted by this interaction (Fs<1.12, ps>.341). These observations parallel the finding in regional thickness differences (described below), where the strongest SES-differences were observed in association regions of the brain.

SES-related differences in regional anatomy across age groups

Prior work has revealed SES related anatomical differences in specific regions of the brain implicated in executive control (e.g., 11, 12), long-term episodic memory (e.g., 13, 14), and verbal ability (e.g., 15) (for review see 16). These observations are consistent with the types of SES-related cognitive differences reported in children (e.g., 17, 18) and adults (e.g., 19, 20).

To explore our primary observations further, we conducted a vertex-wise analysis of SES-thickness relations within each age group across the cortical surface (**Fig. S1**). As this is an exploratory analysis that is meant to supplement and inform the primary finding (focused on mean cortical thickness), relationships are reported using a conventionally lenient threshold (p<.01, uncorrected). As predicted from the observations of mean cortical thickness, the most

prominent positive relationships between SES and gray matter thickness are observable in the earlier-middle age groups (ME): greater cortical thickness was predicted by increasing SES in regions that included the anterior prefrontal cortex, middle-frontal gyrus, ventral anterior cingulate cortex (ACC), posterior cingulate cortex and precuneus (PreCu; **Fig. S1)**. These brain regions are members of various association systems, which are responsible for processes linked to memory, attention and control (9, 10). A number of these regions are also brain regions that are known to exhibit greater anatomical changes during adult aging (e.g., lateral frontal cortex, superior parietal cortex; 21). In addition, SES-relationships were also evident in visual (e.g., middle occipital gyrus) and somatosensory-motor regions (e.g., medial precentral gyrus, postcentral gyrus). In later-middle age (ML), the positive relation between SES and thickness effects were less prominent than ME, but areas that have previously been linked to SES in children (e.g., left IFG; 22) as well as other areas in association systems (e.g., PreCu) exhibited a positive association with SES.

Similar to a previous report that demonstrated younger adults exhibiting a negative correlation between SES (parental education + income) and gray matter volume in the ACC (12), we also found a negative correlation between our SES measure (education + occupation) and the gray matter thickness of the ventral ACC in younger adults. In the older adults, the only significant positive correlation between SES and thickness was found in the anterior insula/frontal operculum, an area implicated in cognitive control (typically a part of the cingulo-opercular control and salience systems; 23, 24). A similar relationship has also previously been reported in older healthy adults, where education is correlated with the thickness in the insula (25).

Altogether, while the regional analyses on functional network organization and brain anatomy are preliminary (and should be tempered with the threshold in the case of anatomical observations), the results suggest that regions involved in executive control and mnemonic processes are particularly susceptible to SES-related effects across adult aging.

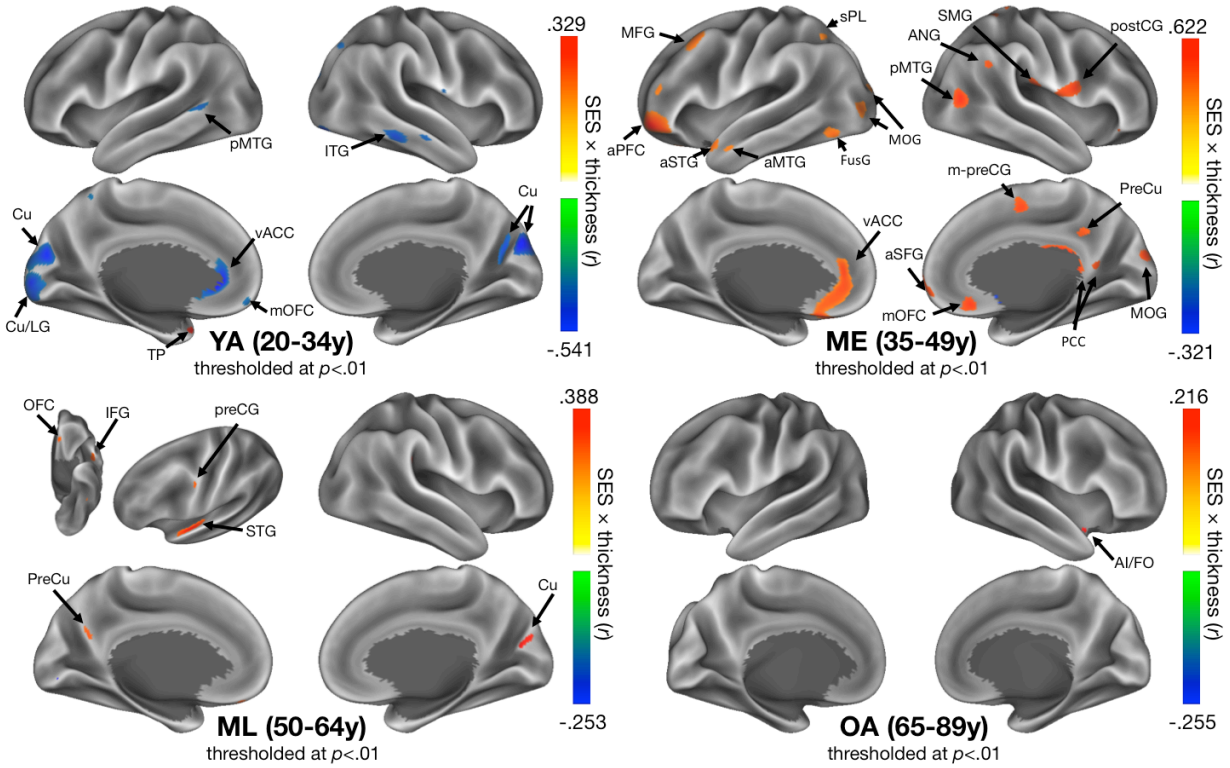

Figure S1 - Regional thickness correlates with SES within each age group. Vertex-wise correlation between SES and gray matter thickness values within each group. Warmer color indicates a positive SES by thickness correlation, whereas cooler color indicates a negative SES by thickness correlation. Correlation maps are thresholded at $p < .01$ (uncorrected) and are depicted on a cortical surface rendering of the brain. Greater SES-related thickness differences shown in ME (see arrows; **YA:** posterior middle temporal gyrus [pMTG], inferior temporal gyrus [ITG], cuneus [Cu], lingual gyrus [LG], ventral anterior cingulate cortex [vACC], medial orbital frontal cortex [mOFC], temporal pole [TP]; **ME:** middle-frontal gyrus [MFG], anterior prefrontal cortex [aPFC], anterior superior temporal gyrus [aSTG], anterior middle temporal gyrus [aMTG], FusG [fusiform gyrus], middle occipital gyrus [MOG], superior parietal lobule [sPL], pMTG, angular gyrus [ANG], supramarginal gyrus [SMG], postcentral gyrus [postCG], vACC, mOFC, anterior superior frontal gyrus [aSFG], medial precentral gyrus [m-preCG], precuneus [PreCu], posterior cingulate cortex [PCC], middle occipital gyrus [MOG]; **ML:** OFC, inferior frontal gyrus [IFG], preCG, superior temporal gyrus [STG], PreCu, Cu; **OA:** anterior insula/frontal operculum [AI/FO]).

1.7. Distributions of SES, cortical thickness, and system segregation across age groups

For both younger and older adults, it is possible that there exist differences in the basic features of the dataset across age groups. However, it is worth pointing out that the absence of SES-related differences in brain anatomy or functional network organization in younger or older adults cannot be easily explained by differences in either number of participants or range/variance of dependent/independent variables across the different age-groups. For example, the older adult group contains the greatest number of participants (n=132) and comparable range and variance of brain measures compared to the middle-early group (Levene's test for homogeneity - segregation: $F(1,173)=0.11$, $p=.743$, OA range=0.28-0.63, $SD=0.07$ vs. ME range=0.41-0.62, $SD=0.05$; cortical thickness: $F(1,173)=2.36$, $p=.126$ OA range=1.99-2.83, $SD=0.13$ vs. ME range=2.23-2.66, $SD=0.11$) and middle-late group (segregation: $F(1,215)=1.33$, $p=.716$, ML range=0.25-0.62, $SD=0.08$; cortical thickness: $F(1,215)=1.86$, $p=.174$, ML range=2.09-2.60, $SD=0.11$). Conversely, the younger adult group (n=44) contains as many participants as the middle-early adult (n=43) group, and comparable range and variance of cortical thickness as the middle-late group ($F(1,127)=2.43$, $p=.121$, YA range=2.36-2.70, $SD=0.08$ vs. ML range=2.09-2.60, $SD=0.11$), and comparable range and variance as the middle-early group ($F(1,85)=2.30$, $p=.132$, YA range=0.42-0.66, $SD=0.05$ vs. ME range=0.41-0.62, $SD=0.05$). Importantly, the range and variance of SES is comparable across all age groups ($F(3,300)=0.058$, $p=.982$).

2. SUPPLEMENTAL METHODS

2.1. Structural imaging acquisition and preprocessing

All brain scans were acquired with a Philips Achieva 3T whole-body scanner (Philips Medical Systems, Bothell, WA) and a Philips 8-channel head coil at the University of Texas Southwestern Medical Center using the Philips SENSE parallel acquisition technique. A T1-weighted sagittal magnetization-prepared rapid acquisition gradient echo (MP-RAGE) structural image was obtained (TR=8.1ms, TE=3.7ms, flip-angle=12°, FOV=204×256mm, 160 slices with 1×1×1mm voxels). The scan duration was 3 minutes 57 seconds.

FreeSurfer v5.3 was used to convert volumetric images into cortical surface representations using the following steps: brain extraction, segmentation, generation of white matter and pial surfaces (**Fig. 1C**), inflation of each surface to a sphere, and surface shape-based spherical registration of the participant's 'native' left and right hemisphere surfaces to the fsaverage surface (26-28). As the participant sample was derived from the adult lifespan, considerable emphasis was placed on quality control and manual editing to diminish sources of potential artifact in the anatomical measurements (i.e., due to instrument noise or head movement; 29). Specifically, automated FreeSurfer outputs were manually inspected for poor skull stripping, inclusions of other tissues (e.g., dura matter, crossing of boundaries between pial and white matter surfaces), vessels or neighboring cortex, and obscuring of the gray and white matter boundary due to insufficient intensity normalization. Our editing procedures involved multiple iterations of editing and verification to minimize the known sources of artifact; we have recently shown how this process improves estimation of age-related differences in measures of brain anatomy (29).

Deformation maps for each individual (one for each brain hemisphere) were generated by combining the (i) deformation maps created when registering an individual's corrected 'native' surfaces to FreeSurfer's fsaverage atlas surfaces, and (ii) the deformation maps for registering fsaverage-aligned data to a hybrid left-right fsaverage atlas (fs_LR; 30). Each individual's corrected 'native-space' FreeSurfer-generated surfaces were then registered to the fs_LR atlas using a single deformation map to limit data resampling.

2.2. Resting-state fMRI acquisition and preprocessing

Participants completed an eyes-open fixation resting-state blood-oxygen-level dependent (BOLD) scan, where they were instructed to stay still and fixate on a white cross-hair presented centrally on a black screen. The experimenter verified that participants complied with the instructions and did not fall asleep during the functional scan via verbal confirmation. The

scans were collected with the following parameters: TR=2000ms, TE=25ms, flip angle=80°, FOV=220mm, 43 interleaved axial slices per volume, 3.5/0mm (slice-thickness/gap), in-plane resolution=3.4×3.4mm. Participants completed either one (154 volumes) or two resting-state scans (180 volumes each). Five volumes were collected at the beginning of each functional scan to allow for T1 stabilization; these 5 volumes were discarded during preprocessing. Importantly, the number of volumes contributing to the analyses was equated across participants, after preprocessing and motion artifact removal (see below).

Standard fMRI preprocessing was used to reduce artifacts through the following steps: slice timing correction, rigid body correction, and realignment. Data were shifted to a mode of 1000 (31). Additional resting-state functional correlation (RSFC)-specific preprocessing steps were applied to reduce spurious variance unlikely to reflect neuronal activity: (i) demean & detrending, (ii) multiple regression of the BOLD data to remove variance related to the whole brain signal, ventricular signal, white matter signal, their derivatives (6 signal regressors derived from eroded FreeSurfer masks), and the 'Friston24' motion regressors (32), and (iii) band-pass filtering (0.009-0.08Hz). To reduce the effect of motion artifacts, a 'scrubbing' procedure was used to flag motion-contaminated resting-state fMRI volumes (i.e., if frame displacement [FD] > 0.3mm). These flagged volumes were replaced with interpolated data for subsequent detrending, nuisance regression and band-pass filtering (i.e., repeating step (i) and (iii); 33). Lastly, the interpolated frames were re-censored in the final data.

The inclusion of global signal regression in resting-state preprocessing has been shown to reduce spatially non-specific signal artifacts such as motion artifacts (33-35). These motion artifacts, if uncontrolled, have been shown to systematically alter the structure of RSFC patterns (35-38). Given that our sample of participants includes older adults with greater motion, with significant correlation between age and mean FD ($r(302)=0.42$, $p<.001$; also seen in past studies; 29, 39, 40), high priority was placed on countering biases in the data by assuring that motion artifacts were removed. While there exists a possibility that genuine neural signals are embedded in the global signal (41), the present study employs a conservative approach to allow confidence in the interpretation of any age-related results. Furthermore, because older adults typically exhibit more motion artifacts, greater amounts of data from older adults were flagged and removed. To ensure that varying amounts of available data across age groups did not influence the results, the number of frames in each participant's data was fixed at 75 frames to maintain a consistent amount of data across the entire sample. Notably, the principle finding (i.e., age group by SES interaction on brain system segregation) remained significant when using all 'clean' frames available in each participant ($F(3,295)=3.95$, $p=.009$, $\eta_p^2=.04$).

Preprocessed resting-state data were registered to the fs_LR (32k) left and right hemisphere surfaces for analysis (27). The participant-specific deformation maps constructed during structural MRI preprocessing were used for one step resampling of the volumetric functional data to the fs_LR surfaces. Lastly, data were smoothed across the surface using a Gaussian smoothing kernel (σ=2.55).

2.3. Nodes and edges definition

Surface-mapped RSFC brain graphs were constructed using a modified set of published nodes (8), in which a node-by-node matrix (i.e., brain graph) was calculated for each participant. The nodes were constructed by (i) identifying the locations of putative area center (each center at least 8mm apart) in a published RSFC-boundary map generated using younger adults data (42) and (ii) 3mm-radius disks were created around the area center to avoid putative boundary locations, which may exhibit more variability across participants (42). A total of 441 nodes were identified across the two hemispheres. Nodes in areas of lower signal intensity (< 800) were identified and discarded using the mean signal intensity map of the data that was used to create the original parcellation (42); this resulted in a final node count of 349 across the two hemispheres (**Fig. 1A**).

The resting-state time series of vertices within each node were averaged together to create a mean time course for each node. The cross-correlation of each node's mean time course was incorporated into a node-to-node correlation matrix. Correlation coefficients were then converted into z-values using Fisher's formula (43), resulting in the final Fisher's z-transformed r-matrix (z-matrix) for each participant (**Fig. 1B**). Due to possible artefactual negative correlations (44, 45) introduced by a necessary processing step used to ensure removal of motion-related artifacts (33, 35), negative z-values were excluded from the data matrix in accordance with past studies (8, 46).

2.4. Brain measures

System-specific Segregation

Segregation of a specific system-type, such as association system segregation, represents the degree to which systems categorized as association systems are segregated from all other functional systems. The segregation of systems from other similar types of systems (i.e., association-to-association system segregation, sensory-to-sensory system segregation), or from other types of systems (i.e., association-to-sensory system segregation, sensory-to-association system segregation) could also be calculated by varying the calculation of between-system connectivity (B_m) in the following formula:

$$Segregation_{sytem-type} = \frac{\overline{W_m} - \overline{B_m}}{\overline{W_m}}$$

where W_m is the mean within-system connectivity of community *m* in a specific system-type (i.e., association, sensory-motor). For overall brain system segregation, such as association system segregation, B_m is calculated as the mean between-system connectivity of each individual association system to all other systems (e.g., connectivity between frontal-parietal task control system to all other systems regardless of system-type). For more specific system-type-to-system-type segregation, such as association-to-association segregation, B_m is calculated as the mean between-system connectivity of each individual association system to all other association systems (e.g., connectivity between frontal-parietal task control system and other association systems). Similarly, for association-to-sensory system segregation, $B_m$is calculated as the mean connectivity between each individual association system to all sensory-motor systems. Once all the $W_m$and B_m are calculated for the individual systems within each system-type, averaged W_m ($\overline{W_m}$) and averaged B_m ($\overline{B_m}$) are used to calculate segregation based on the formula above.

2.5. Measures of demographics, health and cognitive covariates

Demographic covariates

The participants' self-reported race was collected as a six-category variable (i.e., American Indian/Alaskan Native, Asian American/Pacific Islander, Black/African American, Multiracial, Other, White/Caucasian). 84% of the participants were White/Caucasian. The variable was recoded as a binary variable indicating whether or not the participant is a minority (i.e., reporting as non-white/Caucasian). This binary race variable was included along with participant gender as covariates to control for participant demographics.

Physical health covariates

For statistical models that controlled for physical health, covariates included the following measures: subjective physical health (SF-36, physical component score) (47), body mass index (BMI; based on self-reported height and weight), hypertension, smoking-status (binary coding of whether the individual was ever a smoker), alcohol consumption (standard drinks per week), and the presence of chronic physical health issues (i.e., asthma, hepatitis, migraine, encephalitis, heart problem, kidney disease, leukemia, pneumonia, arthritis, ulcers, thyroid problems, other physical illness).

Subjective health was measured using the physical health component score from the SF-36 (47). The SF-36 is a standardized health questionnaire that can differentiate between

different patient groups (48). The physical component score (PCS) is the average of four sub-scales: Physical Functioning, Role-Limitation (physical), Bodily Pain, and General Health. SF-36 was missing from 8 participants. Data were imputed with the sample mean.

The body mass index (BMI) was calculated based on self-reported height and weight. BMI data were missing for 10 participants (i.e., participants did not report exact height or weight). Data were imputed with the sample mean.

Self-reported status of *hypertension* and *smoking status* (i.e., ever a smoker) were coded as binary variables. For alcohol consumption, participants reported approximately how many alcoholic drinks they consumer per week. Lastly, *chronic physical health issues* were coded from a survey completed by participants where they reported whether they experience any of the following chronic issues: asthma, hepatitis, migraine, encephalitis, heart problems, kidney disease, leukemia, pneumonia, arthritis, ulcers, thyroid problems, other physical illness. A participant is coded as 'experiencing chronic health issues' if they reported experiencing one or more of the above chronic health conditions.

Mental health covariates

For statistical models that controlled for mental health, covariates included depressive symptoms, which were assessed using the Center for Epidemiologic Studies Depression Scale (CES-D; 49) and subjective well-being, which was assessed using the Satisfaction With Life Scale (50).

The CES-D was used to measures a participant's depressive symptoms. Scores ranged from 0 to 60, with higher scores indicating more symptoms of depression. Importantly, none of the participants were clinically diagnosed with any depressive disorder at the time of enrollment.

Subjective well-being was measured by the Satisfaction with Life Scale (SWLS; 50), a short 5-item scale that measures life satisfaction (e.g., 'In most ways my life is close to my ideal,' and 'If I could live life over, I would change almost nothing'). It uses a 7 point Likert scale for each item, from 'Strongly Agree' to 'Strongly Disagree'. Responses to the 5 items were averaged to generate life satisfaction score.

Cognitive function covariates

Following procedures from previous work (8), exploratory factor analysis (EFA) was performed on 21 cognitive scores to find the common variance between multiple variables. The number of factors was determined by a quantitative approach, parallel analysis (simulation data = 10000) (51). Three factors were returned, in which two were negatively correlated with age; these factors loaded on to tasks related to episodic memory and fluid intelligence. These two

factors were used as covarites in the present study. See **Table S2** for list of cognitive tasks in episodic memory and fluid intelligence factors.

Cognitive Factors	Cognitive tasks	**Age correlation**
Episodic Memory	Hopkins Verbal Learning Test – Immediate Recall (52) Hopkins Verbal Learning Test – Delayed Recall Hopkins Verbal Learning Test – Recognition Accuracy CANTAB Verbal Recognition Memory – Immediate Recall (53) CANTAB Verbal Recognition Memory – Recognition Accuracy	-0.22, p<.001
Fluid intelligence	Digit Comparison (54) WAIS Digit Symbol (55) FAS (56) Letter Number Sequencing CANTAB Spatial Working Memory CANTAB Spatial Recognition Memory CANTAB Delayed Matching to Sample Operation Span (57) CANTAB Stop Signal Task ETS Card Rotation (58) Raven's Progressive Matrices (59) ETS Letter Sets CANTAB Stocking of Cambridge	-0.72, p<.001

Table S2 – List of cognitive tasks, and age correlation with cognitive factors.

3. SUPPLEMENTAL REFERENCES

1. Adler NE, Epel ES, Castellazzo G, & Ickovics JR (2000) Relationship of subjective and objective social status with psychological and physiological functioning: preliminary data in healthy white women. *Health psychology : official journal of the Division of Health Psychology, American Psychological Association* 19(6):586-592.
2. Gianaros PJ, Marsland AL, Sheu LK, Erickson KI, & Verstynen TD (2013) Inflammatory pathways link socioeconomic inequalities to white matter architecture. *Cereb Cortex* 23(9):2058-2071.
3. Matthews KA, Schwartz JE, & Cohen S (2011) Indices of socioeconomic position across the life course as predictors of coronary calcification in black and white men and women: coronary artery risk development in young adults study. *Soc Sci Med* 73(5):768-774.
4. Schwartz JE (1985) The utility of the cube root of income. *Journal of Official Statistics* 1:5-19.
5. Krishnadas R*, et al.* (2013) Socioeconomic deprivation and cortical morphology: psychological, social, and biological determinants of ill health study. *Psychosom Med* 75(7):616-623.
6. Gianaros PJ*, et al.* (2017) Community Socioeconomic Disadvantage in Midlife Relates to Cortical Morphology via Neuroendocrine and Cardiometabolic Pathways. *Cereb Cortex* 27(1):460-473.
7. Staff RT*, et al.* (2012) Childhood socioeconomic status and adult brain size: Childhood socioeconomic status influences adult hippocampal size. *Ann Neurol* 71(5):653-660.
8. Chan MY, Park DC, Savalia NK, Petersen SE, & Wig GS (2014) Decreased segregation of brain systems across the healthy adult lifespan. *Proc Nat Acad Sci USA* 111(46):E4997-5006.
9. Mesulam MM (1990) Large-scale neurocognitive networks and distributed processing for attention, language, and memory. *Ann Neurol* 28(5):597-613.
10. Posner MI & Petersen SE (1990) The attention system of the human brain. *Annual review of neuroscience* 13:25-42.
11. Gianaros PJ*, et al.* (2007) Perigenual anterior cingulate morphology covaries with perceived social standing. *Social cognitive and affective neuroscience* 2(3):161-173.
12. Yang J*, et al.* (2016) Regional gray matter volume mediates the relationship between family socioeconomic status and depression-related trait in a young healthy sample. *Cogn Affect Behav Neurosci* 16(1):51-62.
13. Janowitz D*, et al.* (2014) Genetic, psychosocial and clinical factors associated with hippocampal volume in the general population. *Translational psychiatry* 4:e465.
14. Wang Y*, et al.* (2016) Pathway to neural resilience: Self-esteem buffers against deleterious effects of poverty on the hippocampus. *Human brain mapping* 37(11):3757-3766.
15. Noble KG, Houston SM, Kan E, & Sowell ER (2012) Neural correlates of socioeconomic status in the developing human brain. *Developmental Sci* 15(4):516-527.
16. Farah MJ (2017) The Neuroscience of Socioeconomic Status: Correlates, Causes, and Consequences. *Neuron* 96(1):56-71.
17. Hackman DA, Gallop R, Evans GW, & Farah MJ (2015) Socioeconomic status and executive function: developmental trajectories and mediation. *Dev Sci* 18(5):686-702.
18. Noble KG, Norman MF, & Farah MJ (2005) Neurocognitive correlates of socioeconomic status in kindergarten children. *Dev Sci* 8(1):74-87.
19. Hurst L*, et al.* (2013) Lifetime socioeconomic inequalities in physical and cognitive aging. *American journal of public health* 103(9):1641-1648.

20. Luo Y & Waite LJ (2005) The impact of childhood and adult SES on physical, mental, and cognitive well-being in later life. *The journals of gerontology. Series B, Psychological sciences and social sciences* 60(2):S93-S101.
21. Raz N*, et al.* (2005) Regional brain changes in aging healthy adults: general trends, individual differences and modifiers. *Cereb Cortex* 15(11):1676-1689.
22. Raizada RD, Richards TL, Meltzoff A, & Kuhl PK (2008) Socioeconomic status predicts hemispheric specialisation of the left inferior frontal gyrus in young children. *NeuroImage* 40(3):1392-1401.
23. Menon V & Uddin LQ (2010) Saliency, switching, attention and control: a network model of insula function. *Brain Struct Funct* 214(5-6):655-667.
24. Seeley WW*, et al.* (2007) Dissociable intrinsic connectivity networks for salience processing and executive control. *The Journal of neuroscience : the official journal of the Society for Neuroscience* 27(9):2349-2356.
25. Liu Y*, et al.* (2012) Education increases reserve against Alzheimer's disease--evidence from structural MRI analysis. *Neuroradiology* 54(9):929-938.
26. Dale AM, Fischl B, & Sereno MI (1999) Cortical surface-based analysis. I. Segmentation and surface reconstruction. *NeuroImage* 9(2):179-194.
27. Fischl B, Sereno MI, & Dale AM (1999) Cortical surface-based analysis. II: Inflation, flattening, and a surface-based coordinate system. *NeuroImage* 9(2):195-207.
28. Ségonne F, Grimson E, & Fischl B (2005) A genetic algorithm for the topology correction of cortical surfaces. *Inf Process Med Imaging* 19:393-405.
29. Savalia NK*, et al.* (2017) Motion-related artifacts in structural brain images revealed with independent estimates of in-scanner head motion. *Human brain mapping* 38(1):472-492.
30. Van Essen DC, Glasser MF, Dierker DL, Harwell J, & Coalson T (2012) Parcellations and Hemispheric Asymmetries of Human Cerebral Cortex Analyzed on Surface-Based Atlases. *Cereb Cortex* 22(10):2241-2262.
31. Ojemann JG*, et al.* (1997) Anatomic localization and quantitative analysis of gradient refocused echo-planar fMRI susceptibility artifacts. *NeuroImage* 6(3):156-167.
32. Friston KJ, Williams S, Howard R, Frackowiak RS, & Turner R (1996) Movement-related effects in fMRI time-series. *Magnetic resonance in medicine* 35(3):346-355.
33. Power JD*, et al.* (2014) Methods to detect, characterize, and remove motion artifact in resting state fMRI. *NeuroImage* 84:320-341.
34. Power JD, Plitt M, Laumann TO, & Martin A (2016) Sources and implications of whole-brain fMRI signals in humans. *NeuroImage*.
35. Satterthwaite TD*, et al.* (2013) Heterogeneous impact of motion on fundamental patterns of developmental changes in functional connectivity during youth. *NeuroImage* 83:45-57.
36. Power JD, Barnes KA, Snyder AZ, Schlaggar BL, & Petersen SE (2012) Spurious but systematic correlations in functional connectivity MRI networks arise from subject motion. *NeuroImage* 59(3):2142-2154.
37. Yan CG*, et al.* (2013) A comprehensive assessment of regional variation in the impact of head micromovements on functional connectomics. *NeuroImage* 76:183-201.
38. Zeng LL*, et al.* (2014) Neurobiological basis of head motion in brain imaging. *Proceedings of the National Academy of Sciences of the United States of America* 111(16):6058-6062.
39. Mowinckel AM, Espeseth T, & Westlye LT (2012) Network-specific effects of age and in-scanner subject motion: a resting-state fMRI study of 238 healthy adults. *NeuroImage* 63(3):1364-1373.
40. Van Dijk KR, Sabuncu MR, & Buckner RL (2012) The influence of head motion on intrinsic functional connectivity MRI. *NeuroImage* 59(1):431-438.

41. Scholvinck ML, Maier A, Ye FQ, Duyn JH, & Leopold DA (2010) Neural basis of global resting-state fMRI activity. *Proceedings of the National Academy of Sciences of the United States of America* 107(22):10238-10243.
42. Wig GS, Laumann TO, & Petersen SE (2014) An approach for parcellating human cortical areas using resting-state correlations. *NeuroImage* 93(2):276-291.
43. Zar J (1996) *Biostatistical Analysis* (Prentice Hall, Upper Saddle River, NJ).
44. Gotts SJ*, et al.* (2013) The perils of global signal regression for group comparisons: a case study of Autism Spectrum Disorders. *Frontiers in human neuroscience* 7:356.
45. Murphy K, Birn RM, Handwerker DA, Jones TB, & Bandettini PA (2009) The impact of global signal regression on resting state correlations: Are anti-correlated networks introduced? *NeuroImage* 44(3):893-905.
46. Power JD*, et al.* (2011) Functional network organization of the human brain. *Neuron* 72(4):665-678.
47. Ware JE, Jr. & Sherbourne CD (1992) The MOS 36-item short-form health survey (SF-36). I. Conceptual framework and item selection. *Medical care* 30(6):473-483.
48. Garratt AM, Ruta DA, Abdalla MI, Buckingham JK, & Russell IT (1993) The SF36 health survey questionnaire: an outcome measure suitable for routine use within the NHS? *Bmj* 306(6890):1440-1444.
49. Radloff LS (1977) A self-report depression scale for research in the general population. *Applied Psychological Measurement* 1(3):385-401.
50. Diener E, Emmons RA, Larsen RJ, & Griffin S (1985) The satisfaction with life scale. *J Pers Assess* 49(1):71-75.
51. Horn JL (1965) A rationale and test for the number of factors in factor analysis. *Psychometrika* 30(2):179-185.
52. Benedict RHB, Schretlen D, Groninger L, & Brandt J (1998) Hopkins Verbal Learning Test Revised: Normative data and analysis of inter-form and test-retest reliability. *Clin Neuropsychol* 12(1):43-55.
53. Robbins TW*, et al.* (1994) Cambridge Neuropsychological Test Automated Battery (Cantab) - a Factor-Analytic Study of a Large-Sample of Normal Elderly Volunteers. *Dementia* 5(5):266-281.
54. Salthouse TA & Babcock RL (1991) Decomposing Adult Age-Differences in Working Memory. *Dev Psychol* 27(5):763-776.
55. Wechsler D (1997) *WAIS-III: Wechsler adult intelligence scale* (Psychological Corporation San Antonio, TX).
56. Bechtoldt HP, Fogel ML, & Benton AL (1962) An Application of Factor-Analysis in Neuropsychology. *Psychological Record* 12(2):147-156.
57. Turner ML & Engle RW (1989) Is Working Memory Capacity Task Dependent. *J Mem Lang* 28(2):127-154.
58. Ekstrom RB, French JW, Harman HH, & Dermen D (1976) Manual for kit of factor-referenced cognitive tests. *Princeton, NJ: Educational Testing Service*.
59. Raven J, Raven JC, & Court JH (1998) *Manual for Raven's Progressive Matrices and Vocabulary Scale* (The Psychological Corporation, San Antonio, TX).